TÜBİTAK

Turkish Journal of Biology

http://journals.tubitak.gov.tr/biology/

Research Article

Turk J Biol
(2017) 41: 302-313
© TÜBİTAK
doi:10.3906/biy-1607-2

The comparison of antioxidant capacity and cytotoxic, anticarcinogenic, and genotoxic effects of Fe@Au nanosphere magnetic nanoparticles

Hande YEĞENOĞLU[1], Belma ASLIM[1], Burcu GÜVEN[2], Adem ZENGİN[3], İsmail Hakkı BOYACI[2], Zekiye SULUDERE[1], Uğur TAMER[4,*]

[1]Department of Biology, Faculty of Science, Gazi University, Ankara, Turkey
[2]Department of Food Engineering, Faculty of Engineering, Hacettepe University, Ankara, Turkey
[3]Department of Chemical Engineering, Faculty of Engineering, Yüzüncü Yıl University, Van, Turkey
[4]Department of Analytical Chemistry, Faculty of Pharmacy, Gazi University, Ankara, Turkey

Received: 02.07.2016 • **Accepted/Published Online:** 01.11.2016 • **Final Version:** 20.04.2017

Abstract: Magnetic gold nanoparticles are used in various biomedical, biochemistry, and biotechnology applications due to their controllable size distribution, long-term stability, reduced toxicity, and biocompatibility. Different coating materials, such as proteins, carbohydrates, lipids, and polyphenols, are applied to enhance the biocompatibility of nanoparticles. In this study, the effects of surface coatings of core-shell structured Fe@Au nanosphere magnetic nanoparticles with regard to antioxidant capacity and cytotoxic, anticarcinogenic, and genotoxic properties were investigated. The obtained results demonstrated that avidin-coated Fe@Au nanospheres had higher antioxidant capacities than uncoated nanospheres. Neither avidin-coated nor uncoated nanoparticles had a cytotoxic effect on normal cells (human gingival fibroblast cell line, HGF-1). In addition, they had anticarcinogenic effects on human cervical carcinoma (HeLa), human breast adenocarcinoma (MCF-7), and human colorectal adenocarcinoma (CCL-221). The genotoxic effects of nanoparticles were also evaluated with DNA tail damage ratio.

Key words: Magnetic gold nanospheres, avidin, antioxidant capacity, cytotoxic, anticarcinogenic genotoxic effects

1. Introduction

Magnetic gold nanoparticles have been increasingly used for the immobilization, concentration, separation, purification, and identification of bioactive agents in analytical biochemistry, medicine, and biotechnology (Yang et al., 2004). They have been preferred in many applications due to their controllable size distribution, long-term stability, and biocompatibility with biomolecules (Xu et al., 2005). During these applications, the main problem with magnetic nanoparticles is the dipole–dipole attractions between them (Song et al., 2015). Surfactants are generally used to provide dispersion stability and prevent aggregation problems. Surface modification changes the physicochemical properties of magnetic nanoparticles; thus, it affects biocompatibility (Guardia et al., 2007), cellular uptake (Song et al., 2015), toxicity (Amin et al., 2015), stability, aggregation, and size. Often used for nanoparticle surface modifications, avidin is a biomolecule and has a high affinity for the small-molecule vitamin biotin (Saleh et al., 2010; Lismont and Dreesen, 2012).

The antioxidant capacity of nanoparticles containing magnetic gold and silver has also been used in various areas. Oxidative stress, a kind of biological damage caused by free radicals, results from metabolic reactions that use oxygen and disturb the balance of prooxidant–antioxidant reactions in living organisms. Oxidative stress occurs due to the increase of reactive oxidative species and decrease of antioxidative systems, and it can lead to tissue damage and several human diseases, such as atherosclerosis, diabetes mellitus, chronic inflammation, neurodegenerative disorders, and cardiovascular diseases (Flora et al., 2007; Vilela et al., 2015). Antioxidants are essential molecules that prevent cell damage by slowing or preventing oxidation (Valko et al., 2007; Pinchuk et al., 2012). Antioxidant capacity is analyzed with various methods, such as spectrophotometric (the determination of total phenolic content with Folin–Ciocalteu reagent), scavenging activity toward stable free radicals (2,2-diphenyl picrylhydrazyl (DPPH)), electrochemical (cyclic voltammetry), amperometric (differential pulse voltammetry), separation techniques (high pressure liquid

* Correspondence: utamer@gazi.edu.tr

chromatography) (Vilela et al., 2015), and the CUPRAC method (Cekic et al., 2015).

The toxicity of nanoparticles was also examined in terms of their cytotoxic, anticarcinogenic, and genotoxic effects. Although magnetic gold nanoparticles have bioconjugation capacities with various molecules, their physicochemical properties might cause cytotoxic effects. It has been reported in the literature that gold nanoparticles induce oxidative stress and toxicity (Tedesco et al., 2010). In another study, Mao et al. evaluated the effect of polycaprolactone coating on the cytotoxicity of gold nanoparticles, and they found that polycaprolactone-coated gold nanoparticles had much less cytotoxicity than bare gold nanoparticles (Mao et al., 2007). It was also pointed out that surface coatings reduce the aggregation and toxicity of magnetic nanoparticles (Lind et al., 2002; Zavisova et al., 2015).

In this study, avidin was chosen for the surface modification of magnetic nanospheres. Biological properties of these nanoparticles were analyzed by examining their antioxidant capacity and cytotoxic, anticarcinogenic, and genotoxic effects. For antioxidant activities, DPPH radical scavenging activity and lipid peroxidation inhibition methods were used. Antioxidant capacities of nanoparticles were also compared with synthetic antioxidants. The cytotoxic and anticarcinogenic effects of nanoparticles were studied on various cell lines (human colorectal adenocarcinoma (CCL-221), human cervical carcinoma (HeLa), human breast adenocarcinoma (MCF-7), and human gingival fibroblast (HGF-1)). In addition, the genotoxic effects of various nanoparticle concentrations were investigated using the comet assay technique. The main objective of the present study was to compare avidin-coated and uncoated Fe@Au nanospheres in biological applications (antioxidant capacity and cytotoxic, anticarcinogenic, and genotoxic effects) and to develop and use biocompatible nanoparticles for cancer treatment. Furthermore, it has been demonstrated that avidin coating enhances antioxidant activity. Coated and uncoated nanoparticles did not show cytotoxic effects on normal cells (HGF-1), although they had anticarcinogenic effects on HeLa, MCF-7, and CCL-221. The genotoxic effects of nanoparticles were determined with human lymphocyte cells and evaluated with the DNA tail damage ratio.

The present study also centered on investigating the effect of avidin coating on Fe@Au nanospheres and determining the antioxidant capacity and cytotoxic, anticarcinogenic, and genotoxic effects of avidin-coated and uncoated Fe@Au nanospheres. The surface and biological properties of both nanospheres were tested for use in safer and more effective chemotherapy. It was presumed that these nanospheres might have the potential to be developed and used as biocompatible nanoparticles for cancer treatment.

2. Materials and methods

2.1. Samples

The three cancer cell lines selected for in vitro antiproliferative bioactivity were derived from colorectal adenocarcinoma, Dukes' type C, (ATCC, CCL-221); human cervical carcinoma, HeLa (ATCC, CRM-CCL-2); and human breast adenocarcinoma, MCF-7 (ATCC, HTB-22). The normal human gingival fibroblast cell line, HGF-1 (ATCC, CRL-2014), was used as a comparative control. The blood samples were obtained from Gazi University Hospital's blood center. Blood lymphocytes were isolated from healthy donors (ages 25 to 30, healthy, not consuming alcohol, nonsmokers, and not on any medication) and they were used for determining the genotoxic effects of nanoparticles.

2.2. Cell cultures and culture medium

Eagle's medium (DMEM) was supplemented with 10% (v/v) heat-inactivated fetal bovine serum, 100 U/mL penicillin, and 0.1 mg/mL streptomycin (with 2 mM L-glutamine for CCL-221, MCF-7, and HeLa; 4 mM L-glutamine for HGF-1) in a humidified atmosphere of 95% air and 5% CO_2 at 37 °C. The medium was changed every 3 days, and the cells were passaged every 5 days. The cells were cultured in flasks and confluent cells were plated at 1×10^4 cells per well of 96-well plates in growth medium. Cells reached about 80% confluency and were then used for the assay. All solutions were prepared with Milli-Q quality water (18 MΩ cm) to reach the desired concentrations.

2.3. Fabrication and preparation of avidin-coated nanoparticles

The gold-coated magnetic spherical nanoparticles (Fe@Au nanospheres) were fabricated using the seed-mediated growth procedure. (Tamer et al., 2010). Briefly, 1.28 M $FeCl_3$ and 0.64 M $FeSO_4.7H_2O$ were dissolved in deionized water. The solution was then stirred vigorously until the iron salts were dissolved. Subsequently, a solution of 1 M NaOH was added dropwise into the mixture by stirring for 40 min, and black precipitated magnetite was obtained. The precipitate was collected with a permanent magnet and washed with deionized water. The resulting iron salt precipitate was first washed in 2 M $HClO_4$ and the particles were then centrifuged for 20 min at 10,000 rpm. Subsequently, the supernatant was discarded, and the particles were washed with deionized water. The washing procedure was carried out in triplicate. The gold shell-coating procedure was carried out with ultrasound in order to encapsulate the iron nanoparticles with gold shells. Iron oxide particles were suspended in an aqueous solution of 0.5 mL of 0.01 M $HAuCl_4$ and stirred for 2 min in the ultrasound. The reaction solution, containing magnetic cores and a reducing agent, 0.01 M $NaBH_4$ (prepared in cold water at approximately 4 °C), was sonicated for 5 min and resulted in a dark red nanoparticle solution.

In order to form a self-assembled monolayer, the surfaces of the Fe@Au nanospheres were modified by leaving them in absolute ethanol containing 20 mM 11-MUA overnight. The nanoparticles were collected with a permanent magnet and washed with 50 mM MES buffer. For surface activation over carboxyl groups, Fe@Au nanospheres were treated with 1 mL of EDC/NHS solution for 40 min. Nanoparticles were separated magnetically and washed twice with 50 mM MES buffer solution. After the activation procedure, the surface was covered with avidin by incubating the nanoparticles in an avidin solution for 40 min to form covalent bonds between avidin and carboxyl groups. Nanoparticles were collected and washed twice with MES buffer. In order to avoid nonspecific interaction, ethanolamine was used and this procedure was carried out for 1 h. The surface washing procedure was repeated twice with phosphate-buffered saline (PBS) solution.

2.4. Determination of antioxidant activities of nanoparticles

Nanospheres at varying concentrations were used in order to determine the antioxidant activity of avidin-coated and uncoated Fe@Au. The antioxidant activities of nanoparticles were analyzed using DPPH radical-scavenging activity and inhibition of plasma lipid peroxidation methods. All experiments were performed at least 3 times.

2.4.1. DPPH elimination method

The radical-scavenging activity of nanoparticles was determined by making some modifications to Blois' method (Blois, 1958). Free radical-scavenging capacities of nanoparticles were measured spectrophotometrically due to the reduced capacity of the methanol solution's effect with DPPH. After the nanoparticles were completely sonicated, their extracted solutions were added to 0.004% DPPH in methanol, and the mixture was shaken forcefully. Next, this mixture was incubated in a horizontal shaker for 30 min at room temperature. After the incubation period, the mixture was centrifuged at 12,500 rpm for 5 min and the nanoparticles were precipitated. After centrifuging, the supernatant was read against a blank in a spectrophotometer at a 517 nm wavelength. The radical inhibition rate (I%) of samples was calculated using the following formula:

$I\% = ([A_{control} - A_{sample}] / A_{control}) \times 100$

$A_{control}$: The absorbance value of the blank.

A_{sample}: The absorbance of the tested sample.

Synthetic antioxidants (BHA, BHT, and α-tocopherol) were used as positive controls.

2.4.2. Inhibition of plasma lipid peroxidation

Inhibition of plasma lipid peroxidation in blood plasma was determined according to the method developed by Rodriguez-Martinez and Ruiz-Torres (1992). Plasma (400 µL), 100 µL of $FeSO_4.7H_2O$ solution (500 µM), 100 µL of H_2O_2 (500 µM), and 200 µL of Fe@Au nanospheres (2 mg/mL) were mixed and incubated for 12 h at 37 °C. After incubation, 375 µL of TCA (4%) and 75 µL of BHT (500 µM) were added and the solution was kept in an ice bath for 5 min. It was then centrifuged at 8000 rpm for 15 min and supernatants were separated from the pellet. 2-Thiobarbituric acid (0.6%, 200 µL) was added to these supernatants. The mixture was stirred vigorously, kept at 95 °C for 30 min, and then cooled. Following that process, 1-butanol was added to the mixture at a 1:1 ratio and the absorbance was measured at 532 nm (Rodriguez-Martinez and Ruiz-Torres, 1992). The lipid peroxidation inhibition activity percentage of samples (I%) was calculated using the following formula:

$I\% = ([A_{control} - A_{sample}] / A_{control}) \times 100$

$A_{control}$: Absorbance value of blank.

A_{sample}: Absorbance value of tested sample.

A blank solution was used as the control group.

2.5. Determination of cytotoxic and anticarcinogenic activities of nanoparticles

2.5.1. Antiproliferation and cytotoxicity assay

The cytotoxic effect of nanoparticles on various cell lines (CCL-221, HeLa, MCF-7, HGF-1) was investigated using a WST-1 Cell Proliferation Assay Kit. The promoting and inhibiting effects of nanoparticles on cell growth were studied in vitro. Different concentrations of avidin-coated and uncoated Fe@Au nanospheres were added to the 96-well plates, each containing 10^4–10^5 cells/plate and 100 µL of DMEM. Each cell was left to incubate for 24 h at 37 °C in a CO_2 incubator, and 10 µL of WST-1 mix was added to each of them. The plate was kept in a horizontal shaker for 1 min and kept in a CO_2 incubator for 2 h again. The absorbance value of plates was read at a 450 nm wavelength in a microplate reader. For the control procedure, the protocol was repeated without cells and absorbance values were obtained. The effects of applied nanoparticle concentrations on liveness of cells were calculated in percentage by using the following formula:

$Liveness\% = (A_{sample} / A_{control}) \times 100$

$A_{control}$: Absorbance value of the blank.

A_{sample}: Absorbance value of the tested sample.

These results were used for calculating the death percentages of cells whose liveness percentages were determined. A healthy cell line (HGF-1) was used as the control group and results of various cancer cell lines (CCL-221, HeLa, MCF-7) were compared to the healthy cell line.

2.5.2. Double staining method

The apoptotic potentials of nanoparticles on MCF-7 and CCL-221 cells were detected by double staining of Hoechst dye with propidium iodide. The apoptotic cells were identified with a fluorescence microscope according to their morphological changes. The double staining method, where apoptotic, necrotic, and live cells exhibit different

radiations under a fluorescence microscope, enables easy differentiation between live and dead cells (Ada et al., 2010). In this method, 100 µg/mL avidin-coated and uncoated Fe@Au nanospheres were used; the highest antiproliferative effects were observed in the MCF-7 and CCL-221 cell lines. The control group consisted of cells treated with cell medium only.

The cells from 6-well plates with 4×10^4–10^6 cell/plate density were applied to 500 µL of particles whose concentrations were adjusted in DMEM. Cells were incubated for 24 h at 37 °C in a CO_2 incubator and washed with PBS. This working solution contained 2 µg/mL Hoechst dye, 1 µg/mL propidium iodide, and 100 µg/mL DNase (not containing RNase). The stain solution was added to the cells and kept at 37 °C for 15 min in a CO_2 incubator for staining. The cells were added to this staining solution and then left to incubate at 37 °C for 15 min in a CO_2 incubator. After incubation, the cells were washed with PBS and observed with a fluorescence microscope (40× magnification). Ada et al. (2010) reported that the Hoechst-stained live cells and apoptotic cells were blue and bright blue, respectively, while necrotic cells stained with propidium iodide were pink. The nuclei of normal cells fluoresced blue at a low intensity, but apoptotic cells exhibited a stronger blue fluorescence.

2.6. Determination of genotoxic effect of nanoparticles

The genotoxic effect of nanoparticles was determined with lymphocytes that were isolated from healthy donor blood. The study protocol was approved by the Ethics Committee of Gazi University (Protocol Number 163/2012). Any DNA damage due to the varying nanoparticle concentrations was investigated by applying the comet technique developed by Singh et al. (1988). This part of the study was conducted in darkness to prevent any additional DNA damage. For this purpose, the blood samples obtained from healthy donors were diluted with PBS buffer at a 1:1 ratio. The lymphocyte isolator Biocoll (2 mL) was added to the mixture and it was centrifuged at 4 °C and 2400 rpm for 20 min. After centrifugation, 2 mL of lymphocytes forming a thin layer at the top of the supernatant was collected to isolate lymphocytes. PBS (2 mL) was added to the 2 mL of lymphocytes, and the mixture was centrifuged at 2400 rpm 20 min. After centrifugation, the supernatant was removed and the pellet was diluted with PBS. The isolated lymphocytes were exposed to various nanoparticle concentrations (0.005–0.100 mg/mL) and incubated at 37 °C for 1 h. After incubation, the mixture was centrifuged at 3000 rpm for 5 min, and the supernatant was removed. Initially, normal melting-point agarose was mounted between the microscope slide and coverslip. The isolated cells were then mixed with low melting-point agarose and added onto the coverslip. The prepared cells were incubated on ice cubes to solidify the agarose parts and the coverslip was taken out carefully. The cells were then submerged in a lysis solution for 1 h. After the lysis step, the microscope slides were held in an electrophoresis tank containing electrophoresis buffer for 20 min to denature the DNA helix. The electrophoresis step was performed at 25 V and 300 mA for 20 min. The microscope slides were then incubated in a neutralization solution at 4 °C for 15 min, and 50 µL of ethidium bromide was dropped on the slides and the slide was covered with a coverslip. The dyed cells were observed with fluorescent microscopy (LEICA DFC425C, Germany) and Comet Analysis Software (version 4.0). DNA damage was calculated using the following formula:

DNA tail damage % = 100 × (tail DNA density / cell DNA density)

A solvent control (PBS), a negative control (untreated), and a positive control (50 µM H_2O_2 for 15 min) were also maintained.

2.7. Statistical analysis

All analyses in this study were carried out with 3 parallels in 3 repetitions and the statistical analyses were performed by one-way analysis of variance (ANOVA) using SPSS 16.0 (SPSS Inc., Chicago, IL, USA). According to Pearson's correlation, the increase of the nanoparticle concentration effects was examined to determine whether there was a correlation with DPPH-scavenging activity, plasma lipid peroxidation, and cytotoxic and genotoxic effects. All obtained data are given as the mean ± SD of 3 independent experiments. The differences among the mean values were determined with Duncan's multiple comparison tests at a confidence level of $P < 0.05$ when significant differences were detected.

3. Results and discussion

3.1. Fabrication of the Fe@Au nanospheres

The prepared Fe@Au nanoparticles were characterized by TEM and UV analysis. As shown in Figure 1, the nanoparticles have a spherical morphology and a mean diameter of 12.5 ± 3 nm. Additionally, the magnetic gold nanoparticles have a plasmon band at 532 nm, which suggests the presence of a gold shell on Fe_3O_4 nanoparticles.

Figure 2 shows that both the 11-MUA-coated and avidin-coated Fe@Au nanoparticles were monodispersed and displayed uniform spherical morphologies with regard to size distribution. The SPR peak of avidin-coated Fe@Au (555 nm) was retained, but different from the 11-MUA-coated Fe@Au magnetic nanoparticles, it displayed a slight red shift of 9 nm. The average hydrodynamic size of the 11-MUA-coated Fe@Au was 8 nm, with a polydispersity index (PDI) of 0.11. After avidin modification, the average hydrodynamic size of avidin-coated Fe@Au increased to 170 nm with a PDI of 0.74. The obtained results confirm that the surface modification of avidin coating affects

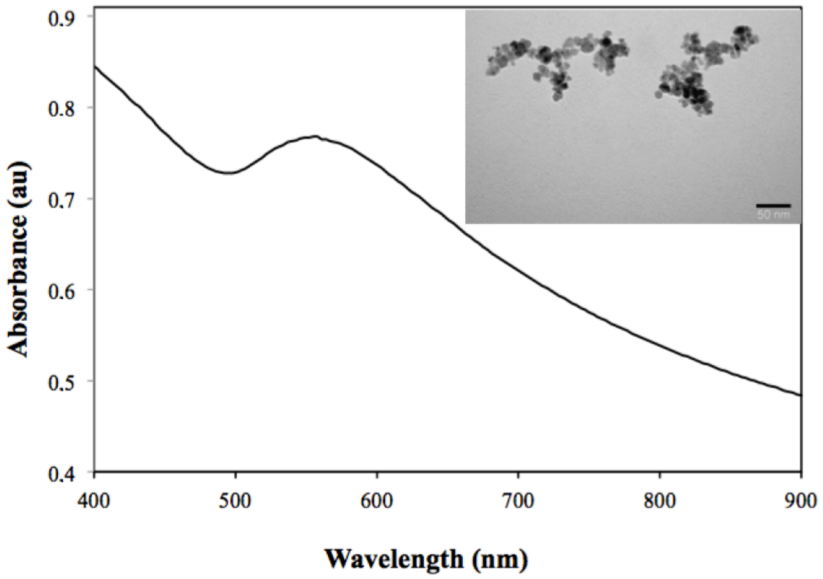

Figure 1. UV spectrum and TEM image of Fe@Au nanospheres.

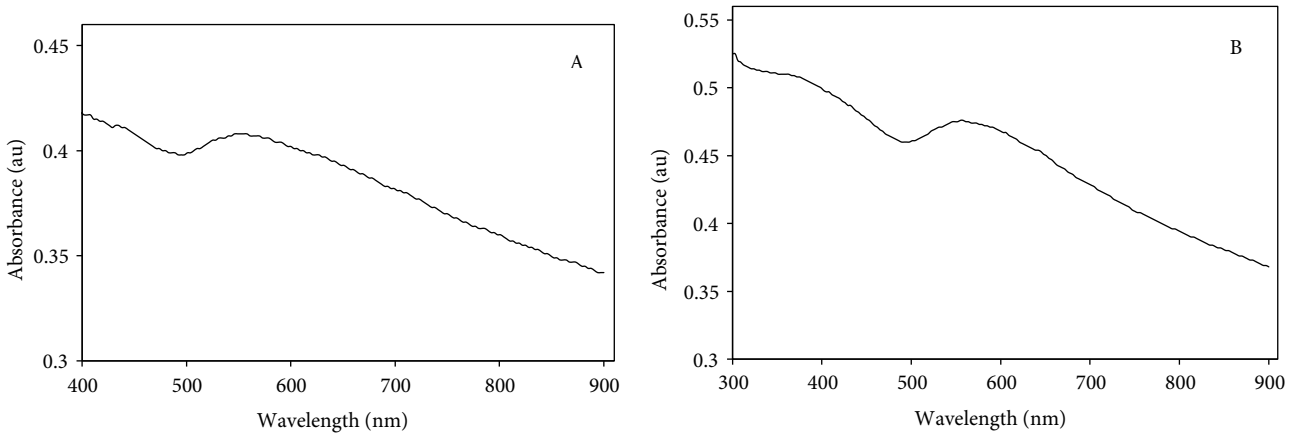

Figure 2. UV spectrum of A) 11-MUA-coated Fe@Au nanospheres and B) avidin-coated Fe@Au nanospheres.

the morphology and monodispersed state of the Fe@Au magnetic nanoparticles. In order to evaluate the surface charge of the magnetic nanoparticles after modification, zeta potential measurements were carried out. The zeta potential values of 11-MUA-coated and avidin-coated Fe@Au magnetic nanoparticles were found to be –6 mV and –12 mV, respectively. The negative increase in the zeta potential value of avidin-coated Fe@Au magnetic nanoparticles suggests that the avidin modification subsequently affects the surface charge of the nanoparticles, as expected.

3.2. Determination of antioxidant activities of nanoparticles

3.2.1. DPPH free radical-scavenging activity

Free radical-scavenging capacities of avidin-coated and uncoated Fe@Au nanospheres were analyzed using DPPH. Avidin-coated nanospheres had more DPPH-scavenging activity, and thus they had an increased antioxidative effect (Table 1). Antioxidant activity was also increased with higher concentrations of avidin-coated nanospheres. When the antioxidant capacities of the highest concentration of nanoparticles (5 mg/mL) were compared, avidin-coated Fe@Au nanospheres had an antioxidant capacity about four times greater than uncoated Fe@Au nanospheres. The results of avidin-coated and uncoated nanospheres were evaluated and found to be statistically different from the control group (synthetic antioxidants) at $P < 0.05$. The obtained result is significant for immunosensor analysis platforms because avidin coating is necessary for designing these analysis platforms. Avidin is used for both sensor designing and antioxidant activity during the fabrication of immunosensor analysis platforms.

Table 1. Comparison of DPPH elimination activities of varying concentrations (0.1, 0.5, 1.0, 5.0 mg/mL) of uncoated and avidin-coated Fe@Au nanospheres. Mean values ± SD, n = 3, different letters (a–d) in the same column are significantly different ($P < 0.05$), different letters (A–C) in the same row are significantly different ($P < 0.05$).

	Percentage of inhibition (%)				
	Fe@Au nanospheres		Synthetic antioxidants		
Concentration (mg/mL)	Uncoated	Avidin- coated	BHA	BHT	α-Tocopherol
0.1	1.4 ± 0.6 ^{a,C}	8.1 ± 0.7 ^{d,B}	94.6 ± 0.8 ^{A}	92.1 ± 0.1 ^{A}	93.7 ± 1.5 ^{A}
0.5	7.6 ± 0.4 ^{b,C}	17.4 ± 0.6 ^{c,B}	96.4 ± 2.1 ^{A}	94.6 ± 2.2 ^{A}	95.9 ± 0.8^{A}
1.0	11.7± 1.6 ^{b,C}	25.8 ± 1.5 ^{b,B}	98.7 ± 1.5 ^{A}	96.1 ± 0.4 ^{A}	96.9 ± 2.2 ^{A}
5.0	17.8 ± 2.1 ^{a,C}	69.1± 2.2 ^{a,B}	99.3 ± 0.6 ^{A}	98.7 ± 0.6 ^{A}	99.8 ± 0.4 ^{A}

Scampicchio et al. (2006) conducted the first study on antioxidant determination during Au nanoparticle synthesis. The growth of Au nanoparticles was obtained from the antioxidant power of polyphenolic-mediated medium by using gold salt, citrate, cetyltrimethylammonium chloride (CTAC), and different concentrations of phenolic acids. Vilela et al. studied the analytical interactions between Au nanoparticles and antioxidant activity (Vilela et al., 2012, 2014). Liu et al. and Andreu-Novorro et al. adopted a similar approach to that of Scampicchio et al. and used CTAB as a stabilizing agent instead of CTAC due to the antioxidant activity in foodstuffs (Scampicchio et al., 2006; Andreu-Navarro et al., 2011; Liu et al., 2012). Apart from these studies, antioxidant activity was also examined during the growth and aggregation of Au nanoparticles (Sudeep et al., 2005; Ma and Qian, 2010). Physicochemical surface coatings and chemical binding also provide no toxic constituents; the coating materials can be removed only by chemical reactions. In the literature, different coating substances, such as gallic, phenolic, tartaric, citric, ascorbic acids, and polyphenols, were chosen. In their study, Andreu-Navarro et al. used several synthetic and natural antioxidant food additives in gold nanoparticle formation, and the antioxidant capacities of modified nanoparticles were analyzed in commercial foodstuff (Andreu-Navarro et al., 2011). It was found that a polymerized form of gallic acid brought antioxidant activity to magnetic nanoparticles (Toth et al., 2014). Trolox was an analogue of vitamin E and functionalized with gold nanoparticles. The functionalized form of Trolox showed a higher antioxidant capacity than its individual form (Nie et al., 2007).

The DPPH-scavenging activity of nanoparticles was also compared with some synthetic antioxidants (BHA, BHT, α-tocopherol). Avidin-coated nanospheres (inhibition: 69.1%) had lower antioxidant capacity than the synthetic antioxidants; however, it is still possible to use avidin-coated Fe@Au nanospheres as an antioxidant in many nanoparticle applications.

3.2.2. Inhibition of plasma lipid peroxidation

Inhibition of plasma lipid peroxidation (%) was evaluated with avidin-coated and uncoated Fe@Au nanospheres, and the obtained results are given in Table 2. The results of avidin-coated and uncoated nanoparticles were analyzed

Table 2. Inhibition of plasma lipid peroxidation activities at different concentrations (0.1, 0.5, 1.0, 5.0 mg/mL) of uncoated and avidin-coated Fe@Au nanospheres. Mean values ± SD, n = 3, different letters (a–c) in the same column are significantly different ($P < 0.05$).

	Lipid peroxidation inhibition (%)	
Concentrations (mg/mL)	Fe@Au nanospheres	
	Uncoated	Avidin-coated
0.1	7.1 ± 0.5 ^{c}	19.3 ± 0.1 ^{c}
0.5	8.5 ± 0.5 ^{c}	21.9 ± 0.4 ^{c}
1.0	23.0 ± 1.4 ^{b}	27.9 ± 1.4 ^{b}
5.0	27.0 ± 0.9 ^{a}	44.8 ± 1.3 ^{a}

and found to be statistically different from the control group (blank solution) at $P < 0.05$. In both nanoparticle types, increasing concentrations resulted in an increased inhibition of plasma lipid peroxidation percentage. Avidin-coated Fe@Au nanoparticles showed the highest activity (44.8%) of lipid peroxidation inhibition. Schaffazick et al. employed a similar method to determine the lipid peroxidation inhibitory effects of nanospheres and nanocapsules containing varying doses of melatonin. Depending on the varying melatonin concentrations (200 and 400 mM), those nanoparticles inhibited lipid peroxidation by amounts ranging from 8% to 51% (Schaffazick et al., 2005).

Avidin-coated nanospheres, in both analysis systems, were found to have a higher inhibition effect than uncoated nanospheres. The results for inhibition of plasma lipid peroxidation were also consistent with DPPH results.

According to these results (radical-scavenging activity and inhibition of plasma lipid peroxidation), avidin-coated Fe@Au nanospheres were found to have better antioxidant capacity than uncoated Fe@Au nanospheres.

3.3. Cytotoxic and antiproliferative effect of nanoparticles

For the cytotoxicity test, a healthy cell culture (HGF-1) and cancer cell lines (CCL-221, HeLa, MCF-7) were used to determine the anticarcinogenic effects of avidin-coated and uncoated nanoparticles. As the obtained results show, the percentage of cell death in healthy gingival cells was lower than the death rates of cancer cell lines.

The nanospheres exhibited moderate cytotoxic activity against all cancer cell lines. On the other hand, the uncoated nanoparticles had the highest antiproliferative effect (34% cell death) on MCF-7 at 0.100 mg/mL. According to the obtained results, the antiproliferative effects on cancer cells of avidin-coated nanoparticles were lower than the effects of uncoated nanoparticles (Table 3). The uncoated nanoparticles displayed anticancer activity against cancer cells and enhanced cytotoxicity on normal cells. The nanoparticle effects were associated with surface coatings. Polysaccharide-coated Ag nanoparticles increased the expression of tumor suppressor proteins, while the uncoated Ag nanoparticles did not. The best concentration for destroying the cancer cells was 0.100 mg/mL of Fe@Au nanospheres, which had the highest cytotoxic effect compared to the other three concentrations (0.005, 0.025, 0.050 mg/mL). The anticarcinogenic and cytotoxic effects of both avidin-coated and uncoated nanoparticles on cancer (CCL-221, HeLa, MCF-7) and healthy (HGF-1) cell lines were investigated. According to statistical analysis, the effects of avidin-coated and uncoated nanospheres on cancer cell lines were examined and observed to be statistically different from the control group (HGF-1) at $P < 0.05$. Nanoparticles seemed to be ineffective on healthy (HGF-1) cell lines, whereas they seemed effective on MCF-7 cell lines at 0.1 mg/mL nanoparticle concentration. The effects of nanoparticle concentration on cancer and healthy cell lines were also investigated in the literature (Chen et al., 2005; Win and Feng, 2005); however, the nanoparticle concentrations used in this study are lower than in other studies in the literature. Finally, avidin-coated and uncoated magnetic Fe@Au nanoparticles were synthesized and studied for anticancer drug-loading and drug-targeting applications. The produced Fe@Au nanospheres led to the death of cancer cells without damaging the healthy cells. All these studies suggest that Fe@Au nanoparticles might be promising novel agents for magnetically targeted drug delivery.

Table 3. Anticarcinogenic and cytotoxic effects of different concentrations (0.005, 0.025, 0.050, 0.100 mg/mL) of uncoated and avidin-coated Fe@Au nanospheres on various cancer (CCL-221, HeLa, MCF-7) and healthy (HGF-1) cell lines. Mean values ± SD, n = 3, different letters (a–e) in the same column are significantly different ($P < 0.05$), different letters (A–E) in the same row are significantly different ($P < 0.05$).

		Percentage of cell death (%)			
Fe@Au nanospheres	Concentration (mg/mL)	HeLa	MCF-7	CCL-221	HGF-1
Uncoated	0.005	$5 \pm 1^{d,BCD}$	$9 \pm 2^{d,A}$	$3 \pm 1^{d,CDE}$	$2 \pm 0^{de,DE}$
	0.025	$12 \pm 1^{c,B}$	$18 \pm 1^{c,A}$	$5 \pm 1^{d,C}$	$5 \pm 1^{cd,C}$
	0.050	$19 \pm 1^{b,CD}$	$30 \pm 2^{ab,A}$	$14 \pm 0^{c,DE}$	$13 \pm 1^{b,DE}$
	0.100	$27 \pm 2^{a,BC}$	$34 \pm 2^{a,A}$	$30 \pm 1^{a,AB}$	$19 \pm 2^{a,DE}$
Avidin-coated	0.005	$6 \pm 1^{d,ABC}$	$7 \pm 1^{d,AB}$	$4 \pm 0^{d,BCDE}$	$1 \pm 0^{e,E}$
	0.025	$11 \pm 1^{c,B}$	$15 \pm 2^{c,AB}$	$11 \pm 1^{c,B}$	$6 \pm 1^{c,C}$
	0.050	$17 \pm 2^{b,CD}$	$26 \pm 1^{b,AB}$	$22 \pm 2^{b,BC}$	$10 \pm 0^{b,E}$
	0.100	$24 \pm 1^{a,CD}$	$32 \pm 2^{a,AB}$	$27 \pm 1^{a,BC}$	$18 \pm 1^{a,E}$

3.3.1. Analysis of apoptotic and normal cells

In the present study, morphological changes and apoptosis in cancer cells were assayed cytologically with Hoechst 33342 and propidium iodide double staining and determined with fluorescence microscope. Avidin-coated and uncoated Fe@Au nanospheres were less cytotoxic on HGF-1 and HeLa cells than on MCF-7 and CCL-221 cells. Because of this, the morphological changes of HGF-1 and HeLa cells were not studied. In other words, avidin-coated and uncoated Fe@Au nanospheres had the highest antiproliferative effects on MCF-7 and CCL-221 cells. The nanospheres showed higher capability to induce apoptosis and morphological changes in cancer cells compared to the untreated control. Apoptotic MCF-7 and CCL-221 cells appeared bright blue in color (yellow arrows) when exposed to avidin-coated and uncoated Fe@Au nanospheres (100 µg/mL), while live cells were light blue (green arrows) in the same area of the micrograph (Figures 3 and 4). In contrast, the control cells showed intact nuclear structures where the cell nuclei exhibited low-intensity blue fluorescence with Hoechst 33342 dye. Exposure to the avidin-coated Fe@Au nanospheres made the induction of apoptosis more obvious than exposure to the uncoated Fe@Au nanospheres. However, the necrotic effects of avidin-coated and uncoated Fe@Au nanospheres on cancer cells were very weak (data not shown). It has been reported that the reaction of particles with cell membranes results in the generation of reactive oxygen species, and the generated oxidative stress may cause a breakdown of membrane lipids, leading to an imbalance of intracellular calcium homeostasis, alterations in metabolic pathways, and finally apoptosis (Clutton, 1997; Knaapen et al., 2004).

3.4. Genotoxic potential of nanoparticles

The genotoxic effects of nanoparticles were determined with human lymphocyte cells and the obtained results are given in Table 4. The major advantage of lymphocytes is that

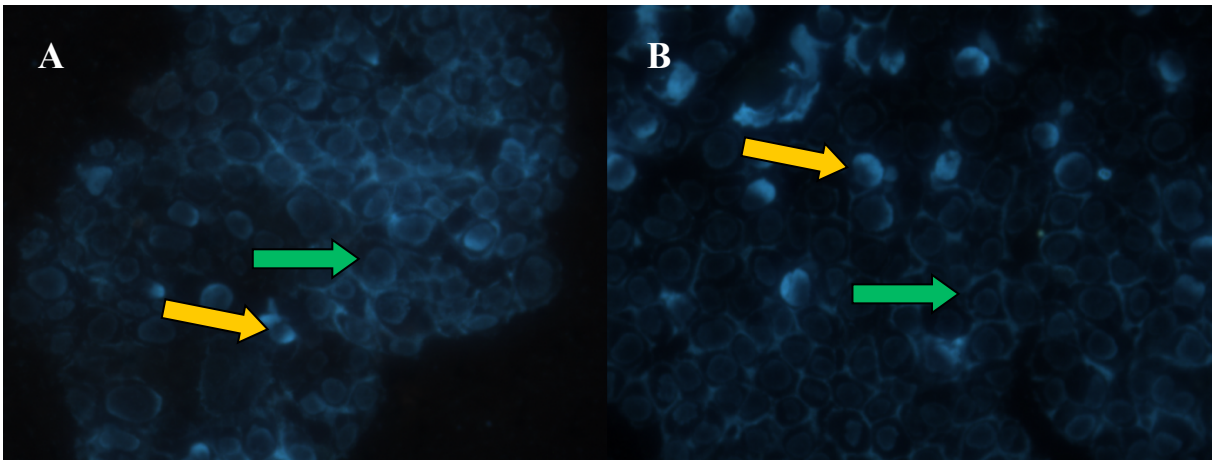

Figure 3. MCF-7 cells under fluorescence microscope using double staining method and 40× magnification after treatment with A) uncoated and B) avidin-coated Fe@Au nanospheres (green arrows: live cells, yellow arrows: apoptotic cells).

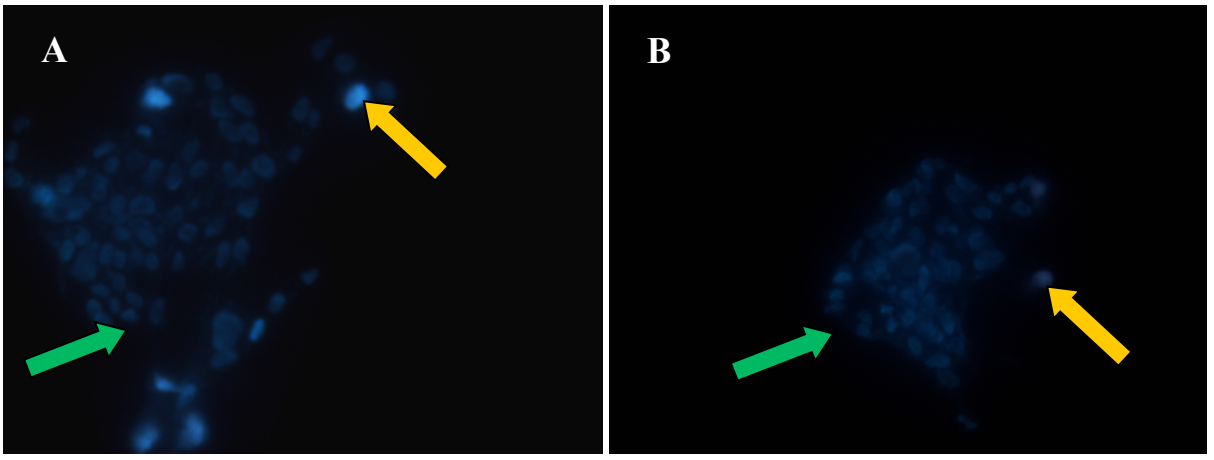

Figure 4. CCL-221 cells under fluorescence microscope using double staining method and 40× magnification after treatment with A) uncoated and B) avidin-coated Fe@Au nanospheres (green arrows: live cells, yellow arrows: apoptotic cells).

Table 4. Potential genotoxic activity of different concentrations of uncoated and avidin-coated Fe@Au nanospheres on human lymphocytes using the comet assay. Mean values ± SD, n = 3, different letters (a–e) in the same column are significantly different ($P < 0.05$).

	Concentration (mg/mL)	Tail length (μm)	Tail moment	Tail DNA damage (%)
Uncoated Fe@Au nanospheres	0.005	30.98 ± 0.27	0.06 ± 0.01	0.35 ± 0.06 [d]
	0.025	31.03 ± 4.49	0.07 ± 0.01	0.41 ± 0.03 [c]
	0.050	30.50 ± 0.70	0.10 ± 0.03	0.54 ± 0.01 [b]
	0.100	32.03 ± 2.88	0.12 ± 0.00	0.66 ± 0.04 [a]
Avidin- coated Fe@Au nanospheres	0.005	32.47 ± 0.12	0.06 ± 0.01	0.34 ± 0.01 [d]
	0.025	33.42 ± 2.95	0.09 ± 0.01	0.38 ± 0.01 [c,d]
	0.050	33.50 ± 0.24	0.15 ± 0.03	0.53 ± 0.04 [b]
	0.100	34.28 ± 2.10	0.12 ± 0.00	0.65 ± 0.01 [a]
Solvent control	-	31.00 ± 2.83	0.02 ± 0.00	0.12 ± 0.02
Negative (untreated) control	-	33.38 ± 2.35	0.02 ± 0.00	0.10 ± 0.02 [e]
Positive control (H_2O_2)	50 mM	32.16 ± 1.73	0.35 ± 0.00	3.05 ± 0.15

they are primary cells and easy to culture in suspension. For this reason, lymphocytes are generally preferred for genotoxicity analysis rather than cell lines (West et al., 1977). Untreated lymphocytes were used as the negative control (DNA damage was 0.10%). Lymphocytes treated only with hydrogen peroxide were used as the positive control (DNA damage was 3.05%). Although there was not enough tail density difference between the control and nanoparticle-treated lymphocyte cells, DNA tail damage increased as the concentrations of nanoparticles increased. Lymphocytes incubated with avidin-coated and uncoated Fe@Au nanospheres caused DNA damage between 0.66% and 0.35%. According to comet test results, if the ratio of tail length to head length is below 5%, it is accepted that there is no DNA damage (Yen et al., 2001). Genotoxic effect results of developed nanoparticles are given in Table 4 and Figures 5A–5C. In the group treated only with hydrogen peroxide, the DNA was completely damaged and the amounts of tail DNA significantly increased (Figure 5C). Untreated (negative control) and nanoparticle-treated lymphocyte cells had no detectable comet tail, whereas cells treated with 50 mM H_2O_2 (positive control) showed significant nuclear DNA fragmentation. The tail DNA of nanoparticle-treated cells (Figure 5A) and untreated cells (Figure 5B) was compared, and it was found that they had similar DNA migration profiles. In addition, statistical analyses were performed, and the results of avidin-coated and uncoated nanospheres were considered to be statistically different from the control group (untreated sample) at $P < 0.05$. The maximum tail DNA damage was 0.66%, which means that the nanoparticles did not induce significant DNA damage compared to the positive controls treated with H_2O_2. Therefore, avidin-coated and uncoated Fe@Au nanospheres did not have genotoxic effects. It was reported in the literature that gold nanoparticles cause death in the carcinoma lung cell line A549, while the BHK21 and HepG2 cell lines remain unaffected (Patra et al., 2007). The toxic effects of gold nanoparticles were observed in in vivo studies using mice, and it was found that 5, 10, 50, and 100 nm gold nanoparticles were not harmful. However, some pathological changes were observed in Kupffer cells. The toxic effects were reduced with peptide-coated gold nanoparticles (Chen et al., 2009). The produced avidin-coated magnetic nanospheres did not have cytotoxic and genotoxic effects, which proved that they are compatible with the human body and can be used for drug manufacturing or diagnosis and detection. These results have important implications for understanding the potential health effects of avidin-coated and uncoated Fe@Au nanosphere exposure.

The results of recent studies suggest that silver and gold nanoparticles reduce the viability of some cancer cells in a dose-dependent manner. Based on these studies, it is hereby speculated that the cytotoxicity of nanoparticles relies on the nature of cell types and size of particles (Park et al., 2011; Gurunathan et al., 2013). Small particles may have good permeability but poor retention. On the other hand, larger particles have higher magnetization and experience higher magnetic forces, which offer better in vivo manipulability in the bloodstream by an external magnetic field for guidance to the tumor. Various particle sizes have been successfully used in clinical trials and in vivo trials with animals, e.g., an average size of 100 nm for magnetic drug targeting (Lubbe et al., 1996). In addition

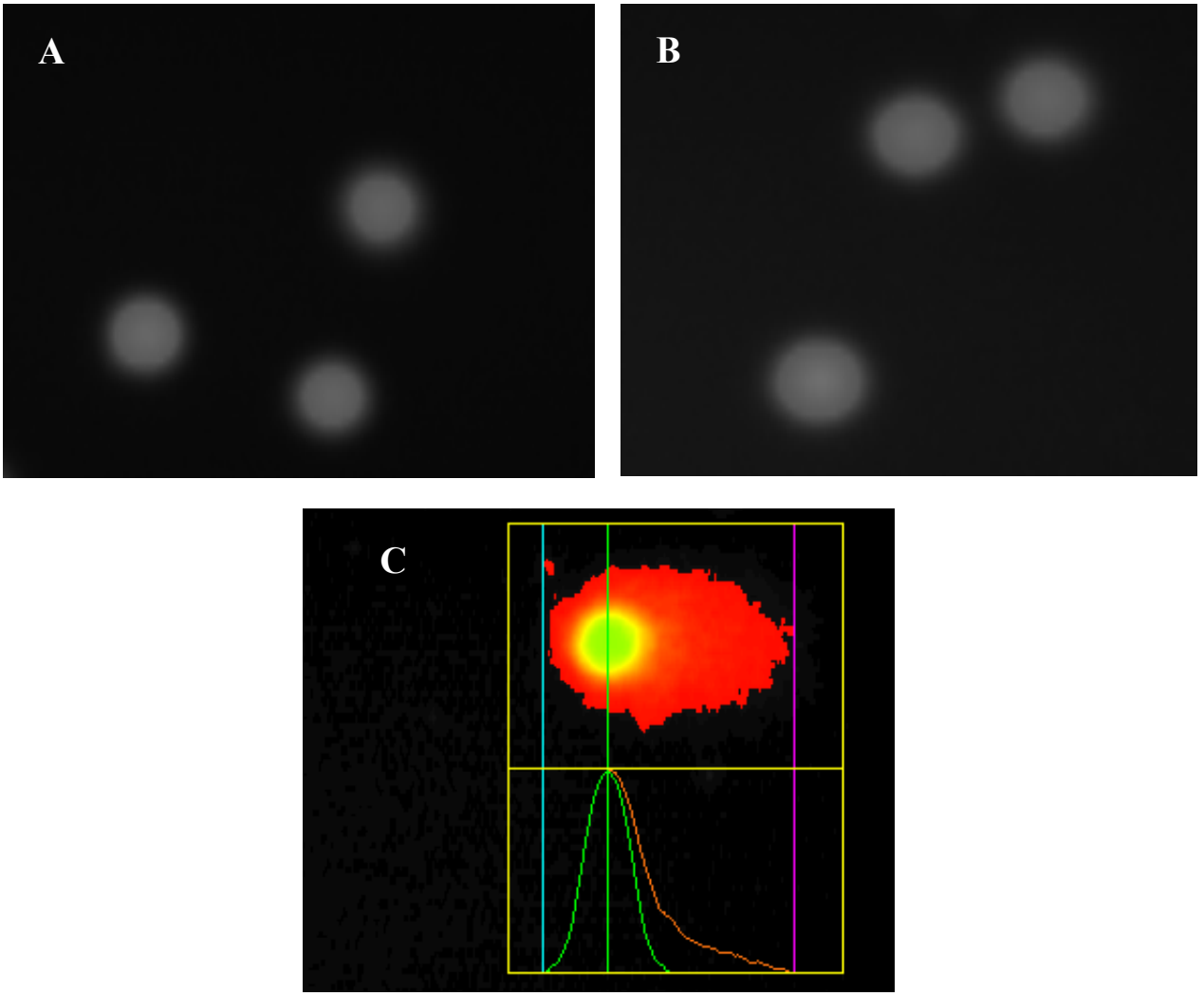

Figure 5. DNA damage in cells after nanoparticle application: A) Nanoparticle-treated lymphocyte cells, B) untreated lymphocyte cells (negative control), C) 50 mM H_2O_2-induced DNA damage and migration (positive control).

to size, surface charge also plays a critical role in blood circulation time of nanoparticles. Positively charged coatings nonspecifically stick to cells at 10^6, whereas the negatively charged particle surface is easily taken up by the liver due to sequestration by phagocytes (Papisov et al., 1993; Fujita et al., 1994). Therefore, it is generally agreed that nanoparticles with a neutral surface experience extended blood circulation times (Sun et al., 2008).

In conclusion, the biological properties of the produced avidin-coated and uncoated Fe@Au spherical nanoparticles were analyzed in terms of their antioxidant capacity and cytotoxic, anticarcinogenic, and genotoxic effects. The importance of surface coating on biological samples was also studied using the avidin molecule. The obtained results revealed that the antioxidant capacity of avidin-coated Fe@Au nanospheres was higher than that of bare nanospheres. Neither avidin-coated nor uncoated nanospheres had cytotoxic effects on healthy cells, but they had strong anticarcinogenic effects on MCF-7 and CCL-221 cells. The genotoxic effects of nanoparticles were evaluated using DNA tail damage value, and avidin-coated and uncoated Fe@Au nanospheres were also found to have no genotoxic effects. The obtained results suggest that such magnetic nanospheres be used in biological applications. These multifunctional nanoparticles may be considered for future nanomedicinal use in simultaneous targeting imaging and real-time monitoring of therapeutic response. Furthermore, due to their reliability, avidin-coated and uncoated Fe@Au nanoparticles may be promising as magnetic drug carrier alternatives for tumor-targeted drug delivery.

Acknowledgment

The authors gratefully acknowledge the financial support from the Gazi University Research Fund through Grant No. 46/2010-02.

References

Ada K, Turk M, Oguztuzun S, Kilic M, Demirel M, Tandogan N, Ersayar E, Latif O (2010). Cytotoxicity and apoptotic effects of nickel oxide nanoparticles in cultured HeLa cells. Folia Histochem Cyto 48: 524-529.

Amin ML, Joo JY, Yi DK, An SSA (2015). Surface modification and local orientations of surface molecules in nanotherapeutics. J Control Release 207: 131-142.

Andreu-Navarro A, Fernandez-Romero JM, Gomez-Hens A (2011). Determination of antioxidant additives in foodstuffs by direct measurement of gold nanoparticle formation using resonance light scattering detection. Anal Chim Acta 695: 11-17.

Blois MS (1958). Antioxidant determinations by the use of a stable free radical. Nature 181: 1199-1200.

Cekic SD, Demir A, Baskan KS, Tutem E, Apak R (2015). Determination of total antioxidant capacity of milk by CUPRAC and ABTS methods with separate characterisation of milk protein fractions. J Dairy Res 82: 177-184.

Chen Q, Espey MG, Krishna MC, Mitchell JB, Corpe CP, Buettner GR, Shacter E, Levine M (2005). Pharmacologic ascorbic acid concentrations selectively kill cancer cells: Action as a pro-drug to deliver hydrogen peroxide to tissues. P Natl Acad Sci USA 102: 13604-13609.

Chen YS, Hung YC, Liau I, Huang GS (2009). Assessment of the in vivo toxicity of gold nanoparticles. Nanoscale Res Lett 4: 858-864.

Clutton S (1997). The importance of oxidative stress in apoptosis. Brit Med Bull 53: 662-668.

Flora SJS, Dikshit M, Flora G (2007). Role of free radicals and antioxidants in health and disease. Cell Mol Biol 53: 1-3.

Fujita T, Nishikawa M, Ohtsubo Y, Ohno J, Takakura Y, Sezaki H, Hashida M (1994). Control of in-vivo fate of albumin derivatives utilizing combined chemical modification. J Drug Target 2: 157-165.

Guardia P, Batlle-Brugal B, Roca AG, Iglesias O, Morales MP, Serna CJ, Labarta A, Batlle X (2007). Surfactant effects in magnetite nanoparticles of controlled size. J Magn Magn Mater 316: E756-E759.

Gurunathan S, Han JW, Kim JH (2013). Green chemistry approach for the synthesis of biocompatible graphene. Int J Nanomed 8: 2719-2732.

Knaapen AM, Borm PJA, Albrecht C, Schins RPF (2004). Inhaled particles and lung cancer. Part A: Mechanisms. Int J Cancer 109: 799-809.

Lind K, Kresse M, Debus NP, Muller RH (2002). A novel formulation for superparamagnetic iron oxide (SPIO) particles enhancing MR lymphography: Comparison of physicochemical properties and the in vivo behaviour. J Drug Target 10: 221-230.

Lismont M, Dreesen L (2012). Comparative study of Ag and Au nanoparticles biosensors based on surface plasmon resonance phenomenon. Mat Sci Eng C-Mater 32: 1437-1442.

Liu QJ, Liu HF, Yuan ZL, Wei DW, Ye YZ (2012). Evaluation of antioxidant activity of chrysanthemum extracts and tea beverages by gold nanoparticles-based assay. Colloid Surface B 92: 348-352.

Lubbe AS, Bergemann C, Riess H, Schriever F, Reichardt P, Possinger K, Matthias M, Dorken B, Herrmann F, Gurtler R et al. (1996). Clinical experiences with magnetic drag targeting: a phase I study with 4'-epidoxorubicin in 14 patients with advanced solid tumors. Cancer Res 56: 4686-4693.

Ma XY, Qian WP (2010). Phenolic acid induced growth of gold nanoshells precursor composites and their application in antioxidant capacity assay. Biosens Bioelectron 26: 1049-1055.

Mao ZW, Wang B, Ma L, Gao C, Shen JC (2007). The influence of polycaprolactone coating on the internalization and cytotoxicity of gold nanoparticles. Nanomed Nanotech Bio Med 3: 215-223.

Nie Z, Liu KJ, Zhong CJ, Wang LF, Yang Y, Tian Q, Liu Y (2007). Enhanced radical scavenging activity by antioxidant-functionalized gold nanoparticles: a novel inspiration for development of new artificial antioxidants. Free Radical Bio Med 43: 1243-1254.

Papisov MI, Bogdanov A, Schaffer B, Nossiff N, Shen T, Weissleder R, Brady TJ (1993). Colloidal magnetic-resonance contrast agents - effect of particle surface on biodistribution. J Magn Magn Mater 122: 383-386.

Park MVDZ, Neigh AM, Vermeulen JP, de la Fonteyne LJJ, Verharen HW, Briede JJ, van Loveren H, de Jong WH (2011). The effect of particle size on the cytotoxicity, inflammation, developmental toxicity and genotoxicity of silver nanoparticles. Biomaterials 32: 9810-9817.

Patra HK, Banerjee S, Chaudhuri U, Lahiri P, Dasgupta AK (2007). Cell selective response to gold nanoparticles. Nanomed Nanotech Bio Med 3: 111-119.

Pinchuk I, Shoval H, Dotan Y, Lichtenberg D (2012). Evaluation of antioxidants: Scope, limitations and relevance of assays. Chem Phys Lipids 165: 638-647.

Rodriguez-Martinez MA, Ruiz-Torres A (1992). Homeostasis between lipid-peroxidation and antioxidant enzyme activities in healthy human aging. Mech Ageing Dev 66: 213-222.

Saleh SM, Muller R, Mader HS, Duerkop A, Wolfbeis OS (2010). Novel multicolor fluorescently labeled silica nanoparticles for interface fluorescence resonance energy transfer to and from labeled avidin. Anal Bioanal Chem 398: 1615-1623.

Scampicchio M, Wang J, Blasco AJ, Arribas AS, Mannino S, Escarpa A (2006). Nanoparticle-based assays of antioxidant activity. Anal Chem 78: 2060-2063.

Schaffazick SR, Pohlmann AR, de Cordova CAS, Creczynski-Pasa TB, Guterres SS (2005). Protective properties of melatonin-loaded nanoparticles against lipid peroxidation. Int J Pharmaceut 289: 209-213.

Singh NP, McCoy MT, Tice RR, Schneider EL (1988). A simple technique for quantitation of low levels of DNA damage in individual cells. Exp Cell Res 175: 184-191.

Song XL, Luo XD, Zhang QQ, Zhu AP, Ji LJ, Yan CF (2015). Preparation and characterization of biofunctionalized chitosan/Fe3O4 magnetic nanoparticles for application in liver magnetic resonance imaging. J Magn Magn Mater 388: 116-122.

Sudeep PK, Joseph STS, Thomas KG (2005). Selective detection of cysteine and glutathione using gold nanorods. J Am Chem Soc 127: 6516-6517.

Sun C, Lee JSH, Zhang MQ (2008). Magnetic nanoparticles in MR imaging and drug delivery. Adv Drug Deliver Rev 60: 1252-1265.

Tamer U, Gundogdu Y, Boyaci IH, Pekmez K (2010). Synthesis of magnetic core-shell Fe3O4-Au nanoparticle for biomolecule immobilization and detection. J Nanopart Res 12: 1187-1196.

Tedesco S, Doyle H, Blasco J, Redmond G, Sheehan D (2010). Oxidative stress and toxicity of gold nanoparticles in Mytilus edulis. Aquat Toxicol 100: 178-186.

Toth IY, Szekeres M, Turcu R, Saringer S, Illes E, Nesztor D, Tombacz E (2014). Mechanism of in situ surface polymerization of gallic acid in an environmental-inspired preparation of carboxylated core shell magnetite nanoparticles. Langmuir 30: 15451-15461.

Valko M, Leibfritz D, Moncol J, Cronin MTD, Mazur M, Telser J (2007). Free radicals and antioxidants in normal physiological functions and human disease. Int J Biochem Cell B 39: 44-84.

Vilela D, Gonzalez MC, Escarpa A (2012). Gold-nanosphere formation using food sample endogenous polyphenols for in vitro assessment of antioxidant capacity. Anal Bioanal Chem 404: 341-349.

Vilela D, Gonzalez MC, Escarpa A (2014). (Bio)-synthesis of Au NPs from soy isoflavone extracts as a novel assessment tool of their antioxidant capacity. RSC Adv 4: 3075-3081.

Vilela D, Gonzalez MC, Escarpa A (2015). Nanoparticles as analytical tools for *in-vitro* antioxidant-capacity assessment and beyond. TrAC-Trend Anal Chem 64: 1-16.

West WH, Cannon GB, Kay HD, Bonnard GD, Herberman RB (1977). Natural cytotoxic reactivity of human lymphocytes against a myeloid cell line - characterization of effector cells. J Immunol 118: 355-361.

Win KY, Feng SS (2005). Effects of particle size and surface coating on cellular uptake of polymeric nanoparticles for oral delivery of anticancer drugs. Biomaterials 26: 2713-2722.

Xu W, Xu S, Ji X, Song B, Yuan H, Ma L, Bai Y (2005). Preparation of gold colloid monolayer by immunological identification. Colloid Surface B 40: 169-172.

Yang HH, Zhang SQ, Chen XL, Zhuang ZX, Xu JG, Wang XR (2004). Magnetite-containing spherical silica nanoparticles for biocatalysis and bioseparations. Anal Chem 76: 1316-1321.

Yen NT, Huang MC, Tai C (2001). Genetic variations of randomly amplified polymorphic DNA polymorphisms in Taoyuan and Duroc pigs. J Anim Breed Genet 118: 111-118.

Zavisova V, Koneracka M, Kovac J, Kubovcikova M, Antal I, Kopcansky P, Bednarikova M, Muckova M (2015). The cytotoxicity of iron oxide nanoparticles with different modifications evaluated in vitro. J Magn Magn Mater 380: 85-89.